Numerical and experimental investigations of water hammers in nuclear industry

R. Messahel[1], B. Cohen[2], M. Moatamedi[3], A. Boudlal[1], M. Souli[1] and N. Aquelet[4]

[1]Laboratoire de Mécanique de Lille, UMR CNRS 8107, USTL, Bd, Paul Langevin, 59655 Villeuneuve d'Ascq Cedex, France
[2]EDF UTO, 1 avenue de l'Europe, 77144, Montévrain, France
[3]Imperial College London, London SW7 2AZ, United Kingdom
[4]Livermore Software Technology Corp., 7374 Las Positas Rd, Livermore CA9455

ABSTRACT

In nuclear and petroleum industries, supply pipes are often exposed to high pressure loading which can cause to the structure high strains, plasticity and even, in the worst scenario, failure. Fast Hydraulic Transient phenomena such as Water Hammers (WHs) are of this type. It generates a pressure wave that propagates in the pipe causing high stress. Such phenomena are of the order of few msecs and numerical simulation can offer a better understanding and an accurate evaluation of the dynamic complex phenomenon including fluid-structure interaction, multi-phase flow, cavitation …

For the last decades, the modeling of phase change taking into account the cavitation effects has been at the centre of many industrial applications (chemical engineering, mechanical engineering, …) and has a direct impact on the industry as it might cause damages to the installation (pumps, propellers, control valves, …). In this paper, numerical simulation using FSI algorithm and One-Fluid Cavitation models ("Cut-Off" and "HEM (Homogeneous Equilibrium Model) Phase-Change" introduced by Saurel et al. [1]) of WHs including cavitation effects is presented.

1. INTRODUCTION

Water Hammers (WHs) are hydraulic transient phenomena. They occur when we modify locally the flow conditions (pump start-up or stop, valve closure) of a fluid contained in a pipe. A shock is generated and is expressed by the discontinuity of the fluid variables (density, pressure, fluid velocity).

In the nuclear power plants, such water hammer occurs in water supply pipes. Due to the high energy and the quantity of water in motion, there is a real threat to the nuclear safety. It can be violent and can cause several damages to the structure (plasticity of pipes and even the rupture of brackets supporting pipes). Those fast dynamic phenomena are of the order of 1e−2 seconds in time, and the actual sensors on nuclear power plants are not accurate enough to capture the pressure wave. Through numerical simulation one can have a better understanding of this complex flow problem.

*Corresponding Author: E-mail: ramzi.messahel@ed.univ-lille1.fr; bernard.cohen@edf.fr; m.moatamedi@imperial.ac.uk; abdelaziz.boudlal@univ-lille1.fr; mhamed.souli@univ-lille1.fr; aquelet@lstc.com

Under certain configuration, the fluid might be put in tension and the local pressure might fall below the saturated vapor pressure giving birth to cavitation, small liquid-free zones ("bubbles" or "voids"). Such phenomena occur most of the time near industrial apparels such as pumps, propellers, impellers and control valves. The rapid collapse of cavitation produces strong shock waves that may harm the interacting structure.

In order to simulate WHs, one needs to consider realistic compressible fluid models that take into account phase change, shock wave generation and its propagation. Among all the existing approaches we can distinguish two major categories.

The first one is the "Two-Fluid Model" [2–4], where each material (liquid and vapor) has its own set of governing equations with additional closing relations and coupling process at the interface between the two materials.

The second one is the "One-fluid Model", where only the average flow is considered by solving a unique set of governing equations and it can be based on a pure phase model (Vacuum Model [5], Cut-off Model [6]) or a mixture model (Saurel et al. Model [1], Isentropic model by Liu [7], Schmidt's model[8]). In the Cut-off pure phase model, the fluid is assumed to be cavitating when it goes below a pre-set cut-off pressure. Such a model is implemented in many commercial softwares, such as LS-DYNA, and was successfully applied to underwater explosions [9] and WHs [10] where the amount of water that is turned to vapor is very small and thus no phase transition is considered. Unlike the Cut-off Model, the phase change model introduced by Bergerat [11] considers phase transition where a unique continuous equation of state is developed for both liquid, vapor and mixture phases based on the sound speed formula given by Wallis [12] and thermodynamic equilibrium. The homogeneous phase change model was successfully implemented and used to solve academic and industrial problems [11]. In this paper, we consider only the barotropic properties of such a model.

Using the FSI capabilities of LS-DYNA, we present in this paper numerical simulation of hydrodynamic ram pressure effects occurring in nuclear industry using the Cut-Off method and the HEM phase-change method presented in [11] when pure phase models cannot be applied.

2. WATER HAMMER'S THEORY

The WH with column separation, also called "the classic WH", has always been in the heart of the research on WHs. Simpson is one of the early pioneers who worked actively on the experimentation of those phenomena. We will simulate the "Simpson's experience" [13] performed in 1986 on the classic WH which provides a good validation case. It contains a complex physic to be modeled: shock wave propagation, cavitation and fluid-structure interaction. A sketch of the experimental setup and the theoretical behavior is given in Figure 1.

Joukowsky and Allievi gave the basis on WH's classical theory through theoretical analysis. The rise of pressure is given by the Joukowsky's equation:

$$\Delta P = \frac{c_L \Delta V}{g}, \tag{1}$$

where C_L is the pressure's wave speed, ΔP is the change of pressure, ΔV is the change of the fluid's velocity and g is the gravitational acceleration.

The wave speed is estimated from Korteweg's equation:

$$C_L = \sqrt{\frac{K/\rho}{1+\left(\frac{K}{E}\right)\left(\frac{D}{e}\right)}}, \tag{2}$$

where K is the bulk modulus, ρ is the mass density, E is the Young's modulus of the pipe wall material, D is the inner diameter and e is the wall thickness.

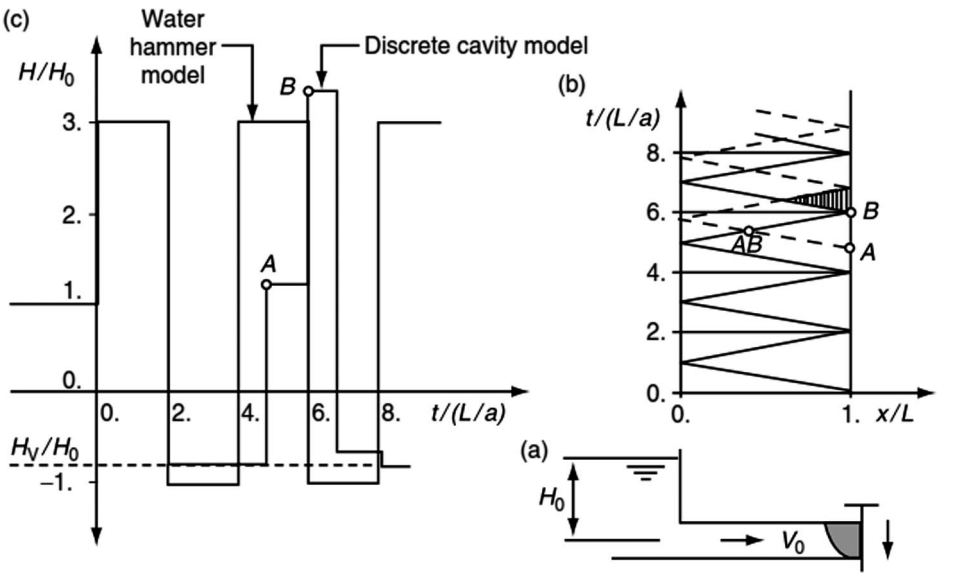

Figure 1: A short duration pressure pulse. (a) Reservoir-pipe-valve system. (b) Wave paths in distance-time plane. (c) Piezometric head history at valve [14]

In this section, we define by $\tau = 2L/C_L$ the time period for a pressure wave to travel back and forth between the valve and the reservoir.

We assume a prescribed velocity at the closed valve as well as a pressure boundary condition at outlet of the reservoir. Thus according to Eqn.1, the change in pressure always occurs at the closed valve, and the change in velocity always occurs at the reservoir.

Let us denote by P_r the pressure in the reservoir, $P_0 = P_r$ the initial pressure, V_0 the initial velocity and t_0 the valve closure time. At time, $t = t_0$, a pressure wave $P = P_1 = P_0 + \Delta P$ is generated at the closed valve ($V = 0$) and is propagated from the valve to the reservoir at the wave propagating velocity c_L.

According to the Eqn. 1, when the pressure wave reaches the reservoir at time $t_0 + \frac{\tau}{2}$, it is reflected due to the prescribed pressure at the reservoir, and thus travels from the reservoir to the valve leaving behind a water at pressure $P = P_r$ and $V = -V_0$ ($V < 0$ because of the pressure gradient $P_1 > P_r$).

When the pressure wave reaches back the valve at time $t = t_0 + \tau$, the confined water in the pipe is entirely at pressure = P_r. The change of velocity ($-V_0$ to 0) generates a pressure drop in the cylinder at the reservoir location maintained at constant pressure P_r, the pressure drop ΔP is given by $P = P_2 = P_r - \Delta P$.

Recalling that $P_0 = P_r$, thus we have $P_2 < P_0$. It leads us to two possible scenarios:

Case 1: $P_2 > P_{sat}$

At time $t = t_0 + \frac{3\tau}{2}$, the pressure wave reaches the reservoir and is once again reflected to the valve.

This time $V = V_2 = V_0$ ($V_2 > 0$, because $P_r > P_2$).

The pressure wave $P = P_r$ reaches the valve at time $t = t_0 + 2\tau$. The entire water is at pressure $P = P_r$, and the new overpressure is $P = P_r + \Delta P_1$. It takes us back to the previous step at time $t = t_0 + \tau$, and we finally have a periodical cycle.

Case 2: $P_2 < P_{sat}$
The pressure at the valve drops to the water vapor pressure. And the new pressure wave is propagated at the liquid vapor pressure.

In order to use Eqn.1 we need to know the new wave propagation velocity depending on the vapor-water mixture.

To go further in the analytical study, we will add the two following hypothesis:

- Only a vapor pocket at the valve is formed during the propagation of the pressure wave from the valve to the reservoir. And we suppose that the size of the vapor pocket is very small compared to the pipe s length. This assumption allows us to consider the pure phase "Cut-off model" that will be considered as a reference solution to validate the "HEM phase-change model".
- The vapor pocket will impose its pressure to the pressure wave as the reservoir does and will act as a fixed pressure boundary condition.

Including the two previous hypothesis, we are able to use Eqn.1. Contrary to the previous case, the reversed direction velocity is no more imposed to be zero but decreases to (Mostowsky 1929)

$$V_0 - \Delta V_{cv} = V_0 - \frac{g(P_r + P_{sat})}{cL}, \tag{3}$$

Now we have a system of two reservoirs (reservoir-vapor cavity). The pressure wave is reflected by the vapor cavity until the vapor pocket collapses a time $t = t_1$, accelerating the water that will impact the valve and give birth to a new WH. The new rise of pressure is less than the first one, but the superposed pressure waves give a greater rise of pressure. In the Figure 1c, the superposition of pressures occurs at time $t = t_0 + 3\tau$.

3. GOVERNING EQUATIONS

3.1 ALE FORMULATION

An ALE formulation contains both pure Lagrangian and pure Eulerian formulations as limit cases. The pure Lagrangian description is the approach, where the mesh moves with the material, making it easy to track interfaces and to apply boundary conditions. Using an Eulerian description, the mesh remains fixed while the material passes through it. Interfaces and boundary conditions are difficult to track using this approach; however, mesh distortion is not a problem because the mesh never changes. In the ALE description, an arbitrary referential coordinate is introduced in addition to the Lagrangian and Eulerian coordinates. The material derivative with respect to the reference coordinate can be described in Eqn. 4. Thus substituting the relationship between the material time derivative and the reference configuration time derivative gives the ALE equation as shown in Eqn. 4,

$$\frac{\partial f(X_i, t)}{\partial t} = \frac{\partial f(x_i, t)}{\partial t} + w_i \frac{\partial f(x_i, t)}{\partial x_i}, \tag{4}$$

Where X_i is the Lagrangian coordinate, x_i the Eulerian coordinate and w_i is the relative velocity. Let denote by v the velocity of the material and by u the velocity of the mesh. In order to simplify the equations we introduce the relative velocity $w = v - u$.

Thus the governing equations for the ALE formulation are given by the following conservation equations as given in Eqn. 5, Eqn. 6 and Eqn. 7:

Mass equation:

$$\frac{\partial \rho}{\partial t} = -\rho \frac{\partial v_i}{\partial x_i} - w_i \frac{\partial \rho}{\partial x_i} \tag{5}$$

Momentum equation:

$$\rho \frac{\partial v_i}{\partial t} = div(\sigma_i) + \rho b_i - \rho w_i \frac{\partial v_i}{\partial x_j} \tag{6}$$

where σ is the stress tensor and boundary and initial conditions need to be imposed for the problem to be well posed.

Energy equation:

$$\rho \frac{\partial E}{\partial t} = \sigma_{ij} v_{i,j} + \rho b_i v_i - \rho w_i \frac{\partial E}{\partial x_j} \tag{7}$$

The term of the relative velocity in Eqn. 5, Eqn. 6 and Eqn. 7 are usually referred to as the advective term, and accounts for the transport of the material past the mesh. It is the additional term in the equations that makes solving the ALE equations much more difficult numerically than the Lagrangian equations, where the relative velocity is zero.

From a discretization point of view of Eqn. 5, Eqn. 6 and Eqn. 7, single point integration is used for efficiency and to eliminate locking. The zero energy modes are controlled with an hourglass viscosity, see Aquelet et al [15]. A shock viscosity with linear and quadratic terms derived by Von Neumann and Richtmeyer [17] is used to resolve the shock wave. A pressure term is added to the pressure in the energy Eqn.7. The resolution is advanced in time with the central difference method, which provides a second order accuracy in time using an explicit method. For each node, the velocity is updated as shown,

$$u_{n+\frac{1}{2}} = u_{n-\frac{1}{2}} + \alpha \Delta t \tag{8}$$

Where $\alpha = \frac{F_{ext} + F_{int}}{M}$, M, F_{ext} and F_{int} are respectively the nodal acceleration, the nodal mass, the nodal mass, the external forces and the internal nodal forces.

3.2 CONSTITUTIVE MODEL AND EQUATION OF STATE

The water, the vapor and the mixture are governed by the same constitutive material model given by

$$\sigma = -P.Id + \tau, \text{ where } \tau = \mu \dot{\varepsilon} \tag{9}$$

Where μ and $\dot{\varepsilon}$ respectively denote the dynamic viscosity and the strain in rate form. The pressure term is calculated using an adequate equation of state that expresses the relation between the density, the pressure and the internal energy.

It is through this equation of state that both "Cut-Off" and "Phase-Change" cavitation models are defined.

3.2.1 Cutoff Model

The Cutoff Model is a pure phase model assuming that cavitation occurs when the local pressure reaches or goes below a predefined Cutoff pressure P_{cutoff} and the pressure is thus

simply set to $P = P_{cutoff}$. Any classical equation of state for water can be used to define the thermodynamic properties of water for pressures above the lower P_{cutoff} limit. A Linear Polynomial equation of state is used:

$$P = C_0 + C_1\mu + C_2\mu^2 + C_3\mu^3 + (C_4 + C_5\mu + C_6\mu^2)E \tag{10}$$

Where C_0, C_1, C_2, C_3, C_4, C_5 and C_6 are the linear polynomial coefficients, μ and E are the specific relative volume and specific energy. Variables are set to be $C_0 = C_2 = C_3, C_4 = C_5 = C_6 = E = 0$ whereas $C_1 = K$ the bulk modulus of the water in order to recover the barotropic linear in density equation:

$$P = \begin{cases} c^2(\rho - \rho_0), P > P_{cutoff} \\ P_{cutoff}, P \leq P_{cutoff} \end{cases} \tag{11}$$

3.2.2 Phase-Change Model

The phase-change cavitation model considered in this paper is from the family of HEM (Homogeneous Equilibrium Model) one-fluid equations of state. From the formulations presented by Bergerat [11], we consider in this paper only the barotropic properties of the fluid.

The phase change cavitation model was originally proposed by Saurel et al. [1]. Three different phases are considered in this model: the pure water phase, the mixture phase and the pure vapor phase. We define at constant temperature and at the boundary of the phases the thermodynamic variables at the saturation state:

- The density of the liquid at saturation: $\rho_{sat,l}$
- The density of the vapor at saturation: $\rho_{sat,v}$
- The saturated pressure: P_{sat}

The mixture density is defined by: $\rho = \alpha\rho_{sat,v} + (1 - \alpha)\rho_{sat,l}$ where:

$$\alpha = \frac{\rho - \rho_{sat,l}}{\rho_{sat,v}, \rho_{sat,l}} \tag{12}$$

In HEM model, the thermodynamic and mechanical fluid at saturation is considered at equilibrium such that:

$$P_{sat} = P(\rho_{sat,l}) = \mathrm{P}(\rho_{sat,v}) \tag{13}$$

In order to guarantee the continuity in density when the fluid passes from one phase to another. The linear in density equation of state (Eqn. 11) for the liquid phase and the ideal gas equation for the vapor has been rearranged such that eq.13 is always verified. The pressure is finally given by:

$$P = \begin{cases} P_{sat} + c_{liq}^2(\rho - \rho_{sat,l}), & \rho > \rho_{sat,l} \\ P_{sat}, & \rho_{sat,v} \leq \rho \leq \rho_{sat,l} \\ \rho_{sat,v}\, c_{vaq}^2/\gamma, & \rho \leq \rho_{sat,v} \end{cases} \tag{14}$$

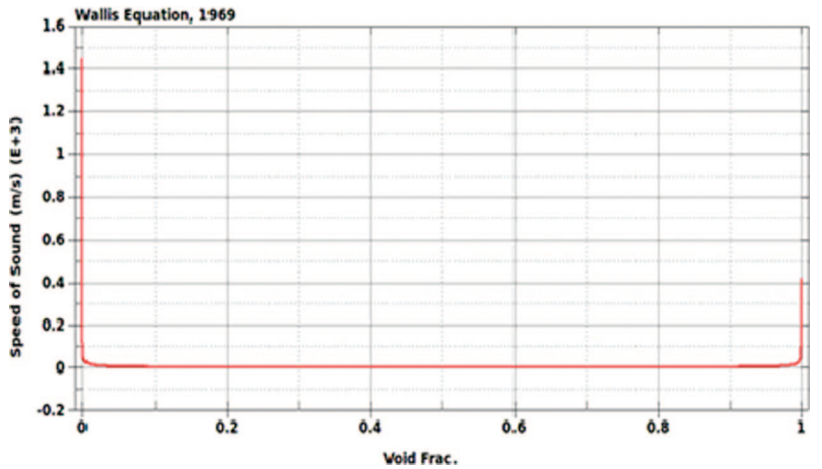

Figure 2: Speed of sound for water mixture phase according to Wallis formula 1969 [12]

The speed of sound for the mixture (liquid-vapor) phase is computed from theoretical sound speed formula given by Wallis [12]:

$$c = \sqrt{[\alpha\rho_{sat,v} + (1-\alpha)\rho_{sat,l}] \cdot \left[\frac{\alpha}{\rho_{sat,v}\ c_{vap}^2} + \frac{(1-\alpha)}{\rho_{sat,l}\ c_{liq}^2}\right]}, \tag{15}$$

Figure 2 illustrates the application of Eqn.12 and Eqn.16 to water material at 20°C.

4. NUMERICAL SIMULATIONS

4.1 SIMPSON'S EXPERIMENT [13]

4.1.1 Numerical setup

Simpson's experience [13] was made in 1986. It is a WH due to the rapid closure of a valve and is described in section 2. The main objective of this experiment is to show the need of taking into account the elasticity of the pipe through the coupling effects between the structure and the fluid, the study of the short duration pressure pulse, its impact on the structure and finally the cavitation effects that is generated near the valve and its condensation leading to a second shock wave. We will present two simulations, made on LS-DYNA, of the dispositive drawn in Figure 1a.

A first one dimensional simulation is performed in order to highlight the consequences of neglecting the elasticity of the pipe and the fluid-structure interaction effects (over-estimation of the pressure peak, over-estimation of the celerity of the pressure wave, ...) and the validation of HEM phase-change model compared to the cut-off model. Since only a small amount of void fraction is created at the end of the pipe (closed valve), the hypothesis given in section 2 (for analytical study) justify the use of a pure phase Cut-off model and the validation of both Cut-off and HEM phase change cavitation models for the valve slam WH. The full model is composed of 67600 ALE hexahedra elements. The flow is constrained to be 1D setting the velocity in Y-direction and Z-direction to be equal to zero. The same strategy is used to model the closed valve at the end by imposing a zero velocity at the nodes at the end of the pipe.

A second three dimensional simulation will be performed using the HEM phase-change cavitation models and the LS-DYNA fluid-structure interaction coupling algorithm. The obtained

results will be validated in comparison with the experimental and the WAHA code [18], a code designed and validated for the simulation of WHs in elastic pipes. The full model is composed of 216000 hexahedra ALE elements for the water, 120 hexahedra ALE elements for the reservoir and 86400 Belytschko-Lin-Tsay type [19] four nodes shell elements for the structure.

Sketches of the meshes are shown in Figure 3 and Figure 4 for both one-dimensional and three-dimensional simulations.

For performance CPU time, a Lagrangian coupling, where fluid nodes and structure nodes are commonly used at the fluid-structure interface, where fluid mesh is not highly distorted. We will take into account the coupling effects by merging the nodes between Lagrangian (Structure) and ALE (Fluids) parts. Common nodes of a Lagrangian and ALE mesh will be considered Lagrangian and constitute a boundary condition for the ALE mesh (material velocity = mesh velocity).

The parameters for the experimental setup are given in Table 1 and the parameters for material models and equations of state (IAPWS [20]) are given in Table 2, Table3, Table 4 and Table 5.

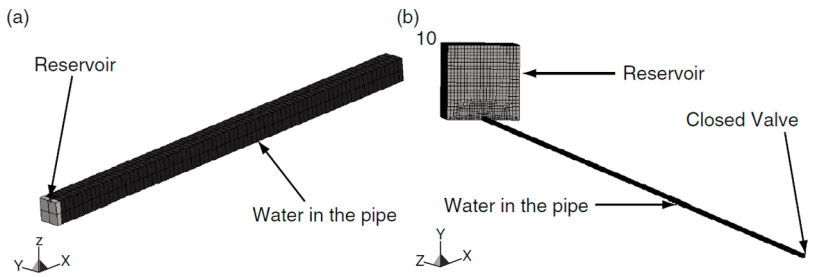

Figure 3: Sketch of the mesh of the 1D model

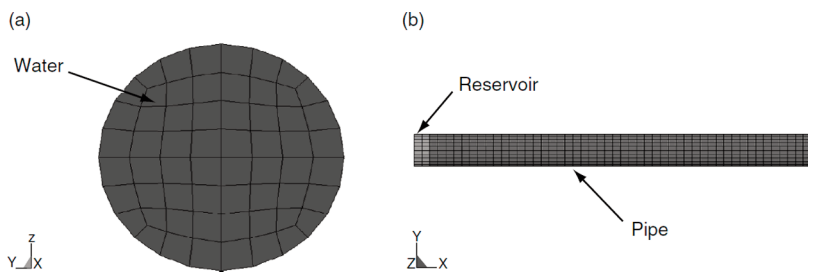

Figure 4: Sketch of the mesh of the 3D model (the model is truncated at the right side)

Table 1: Simpson's Experience parameters. (a) Initial conditions. (b) Pipe's geometry and material characteristics. [21]

(a)		**(b)**	
Pressure (MPa)	3.419	Inside Diameter (mm)	19.05
Temperature (C° degree)	23.3	Thickness (mm)	1.6
Velocity ($m.s^{-1}$)	0.4	Elastic Modulus (GPa)	120
		Length (m)	36

Table 2: MAT_ELASTIC parameters

Pipe	RO	E	PR	DA	DB	K
	8960	1.2e + 11	0.355	0.0	0.0	0.0
			VC	**CP**		
			None	1.0e + 20		

RO: Mass Density, E: Young's Modulus, PR: Poisson's ratio, DA: Axial Damping Factor, DB: Bending damping factor, K: Bulk Modulus, VC: Tensor viscosity coefficient, CP: Cavitation Pressure.

Table 3: MAT_NULL parameters

Water	RO	PC	MU	TEROD	CEROD	YM	PR
	997.58	−10.0	0.0	0.0	0.0	0.0	0.0

RO: Mass density, PC: Pressure cutoff, MU: Dynamic viscosity coefficient, YM: Young's Modulus, TEROD: Relative volume for erosion in tension, CEROD: Relative volume for erosion in compression, PR: Poisson's ration.

Table 4: EOS_LINEAR_POLYNOMIAL parameters

Water	C0	C1	C2	C3	C4	C5	C6
	0.0	2.02E+9	0.0	0.0	0.0	0.0	0.0
	E_0	V_0					
	0.0	0.999845					

C0, C1, C2, C3, C4, C5, C6: User-defined constants. E_0: Initial internal energy per unit reference volume, V_0: Initial relative volume.

Table 5: EOS_PHASE_CHANGE parameters

MIXTURE	RLIQ	RVAP	CLIQ	CVAP	PSAT	V0
	997.497	0.0205983	1491.03	425	2.81e+3	0.999846

RLIQ: Saturated Liquid's density. *RVAP:* Saturated Vapor's density. *CLIQ:* Speed of Sound for liquid *CVAP:* Speed of Sound for vapor. *PSAT:* Saturated pressure V_0: Initial relative volume.

4.1.2 Numerical results

Results for the first one-dimensional simulation are shown in Figure 5 in term of pressure time history of the fluid at the closed valve. The blue, green and red curves represent respectively the LS-DYNA HEM phase-change results, the LS-DYNA cut-off results and the experimental results. Analyzing Eqn. 2 and considering that one-dimensional simulation is equivalent to three-dimensional simulation with a stiff pipe (very high young modulus) we find that the simulated wave propagation speed c_L is equal to the speed of sound of the water. One can also see in Eqn.2 that the more the pipe is elastic and the more the wave propagation speed is low. Replacing in Eqn. 1 c_L by the speed of sound and comparing the LS-DYNA results to the experimental result we can verify in Figure 5. the analytical study and that the pressure peak and the wave speed propagation are over-estimated neglecting the elasticity of the pipe and fluid-structure coupling effects. Comparing the "cut-off " and the "HEM phase-change" models we can see the good correlation between the two models. One may notice the oscillations occurring at time $t = 0.12s$ when the vapor pocket located at the valve condensates, it can be explained by the huge change in speed of sound in the mixture fluid when the void fraction is very small and tends to zero (see Figure 2) as a direct consequence

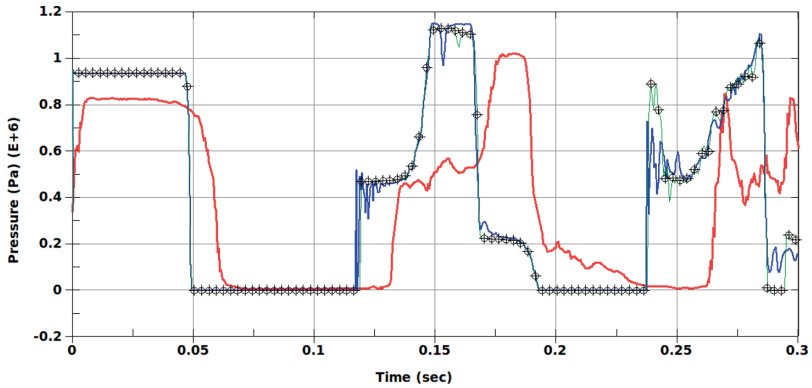

Figure 5: Pressure time history at the closed valve for the one-dimensional simulation. The blue, green and red curves represent respectively the LS-DYNA HEM phase-change results, the LS-DYNA cut-off results and the experimental results

of the use of Eqn.15 for the computation of the speed of sound and the bulk modulus of the fluid.

Results for the second three-dimensional simulation are shown in Figure 6 in term of pressure time history of the fluid at the closed valve. The blue, green and red curves represent respectively the LS-DYNA HEM phase-change results, the WAHA elastic results (1d simulation with correction of the wave propagation speed by Eqn. 2) and the experimental results. Pressure values from LS-DYNA simulation have been compared to both experimental data and WAHA code results, and good correlations have been observed considering explicitly the fluid-structure strong coupling and the elasticity of the pipe and considering implicitly it effects on the pressure peak and the wave propagation speed through Eqns 1and 2. The monophase WH is well simulated according to the first pressure peak in Figure 6, while the

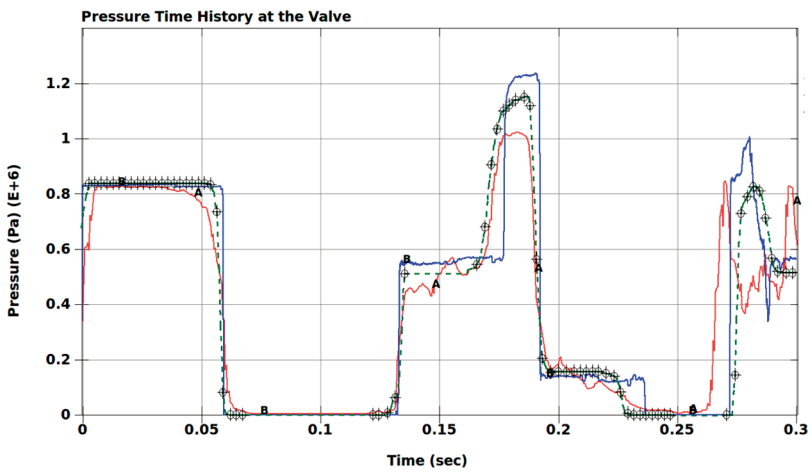

Figure 6: Pressure time history at the closed valve for the three-dimensional simulation. The blue, green and red curves represent respectively the LS-DYNA HEM phase-change results, the reference Waha code for WHs simulation results and the experimental results

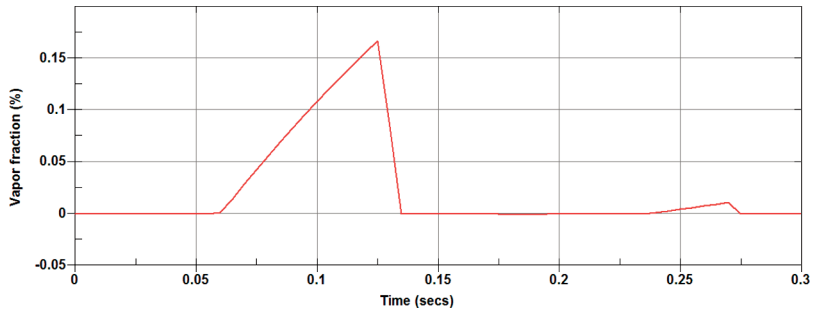

Figure 7: Void Fraction computation using the LS-DYNA HEM phase-change model at the valve for Three-dimensional simulation with fluid-structure interaction

second one due to the brutal condensation of the water steam pocket is slightly over-estimated. One may notice that considering the fluid-structure interaction the pressure wave propagation speed is well recovered.

In Figure 7, we show through the void fraction that the different stages of the phase change phenomenon has been model: Its generation as liquid water turns to saturated vapor ($0 < \alpha < 1$) followed by its condensation as saturated vapor turns to liquid water ($\alpha \leq 0$).

4.2 COLD WATER HAMMER TEST FACILITY EXPERIENCE (CWHTF): WAHALOAD PROJECT [22]

4.2.1 Numerical setup

The Cold Water Hammer Test Facility (CWHTF) was designed and built at Forschungszentrum Rossendorf for the WAHALoad European project [23] in order to study the fluid structure interaction effects during the WH phenomenon due the sudden condensation of a saturated vapor pocket.

This test case is chosen to investigate the performance of the presented phase change model for the simulation of WH where the classical pure phase model such as the cut-off model cannot be used due to initial presence of a non-negligible amount of saturated vapor pocket. The experimental setup sketch and picture is shown in Figure 8, and is composed of a water tank, a pipe equipped, a closed end (rigid disk) and a valve in the middle of the pipe that separates the pipe into two parts: a left one linked to the lank and a right one linked to the closed end (see Figure 8).

At the beginning the valve is opened and the pipe is entirely filled with cold water at the atmospheric pressure. Then the valve is closed and the remaining air is evacuated in t he right part such that only liquid water and steam at saturation is remaining at the right part. So far we have: the water tank and the left part of the pipe at the atmospheric pressure and the right part of the pipe composed of liquid water at the saturation pressure and above a vapor pocket at saturation pressure closed to the end. This is the initial setup for our simulation.

At time t = 0 sec, the valve is opened and due to the difference in pressure between the left and the right part the liquid water is accelerated in the direction of the closed end, compressing the vapor pocket until it collapses and triggers the WH.

The finite element mesh is shown in Figure 9 where the red elements represent the water tank, the blue element the liquid water at atmospheric pressure, the green elements the liquid water at the saturation pressure and the yellow elements the initial saturated water steam. The structure is modeled by Belytschko-Lin-Tsay under integrated shell elements. The fluid structure coupling method is the same than the one described in the previous section.

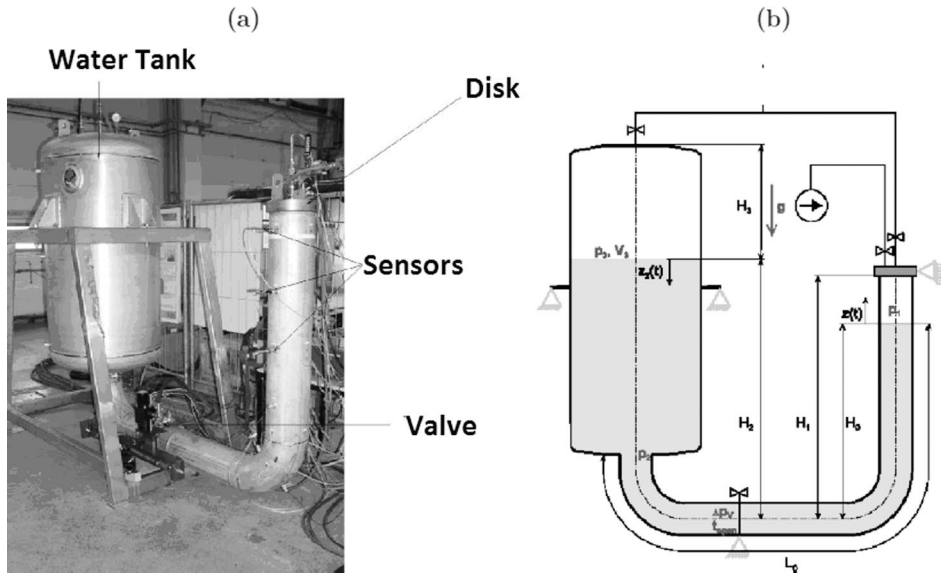

Figure 8: Water Hammer Test Facility Built for the WAHALoad Project [22]

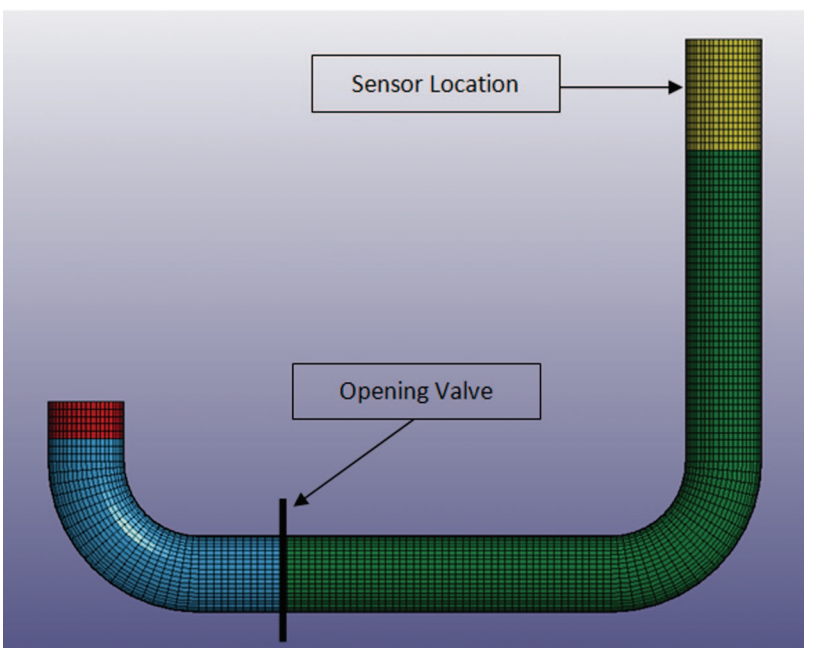

Figure 9: LS-DYNA Mesh where the water tank is in red, the initial liquid water at 1 bar in blue, the initial liquid water at saturation in green and the saturated water steam in yellow

The parameters for the experimental setup are given in Table 6 and the parameters for material models and equations of state (IAPWS [20]) are given in Table 7, Table 8, Table 9 and Table 10.

4.2.2 Numerical results

Results for the first CWHTF simulation is shown in Figure 10 in term of pressure time history of the fluid at the sensor location (see Figure 9). The blue and red curves represent

Table 6: CWHTF parameters. (a) Initial conditions. (b) Pipe's geometry and material characteristics. [22]

(a)		**(b)**	
Atmospheric Pressure (bars)	1.0	Inside Diameter (mm)	207
Temperature (C° degree)	23.3	Thickness (mm)	6
		Elastic Modulus (GPa)	210
		Length (m)	3.285

Table 7: MAT_ELASTIC parameters

Pipe	**RO**	**E**	**PR**	**DA**	**DB**	**K**
	7850	2.1e + 11	0.3	0.0	0.0	0.0
			VC	**CP**		
			None	1.0e + 20		

RO: Mass Density, E: Young's Modulus, PR: Poisson's ratio, DA: Axial Damping Factor, DB: Bending damping factor, K: Bulk Modulus, VC: Tensor viscosity coefficient, CP: Cavitation Pressure.

Table 8: MAT_NULL parameters

Water	**RO**	**PC**	**MU**	**TEROD**	**CEROD**	**YM**	**PR**
	997.58	−10.0	0.0	0.0	0.0	0.0	0.0

RO: Mass density, PC: Pressure cutoff, MU: Dynamic viscosity coefficient, YM: Young's Modulus, TEROD: Relative volume for erosion in tension, CEROD: Relative volume for erosion in compression, PR: Poisson's ration.

Table 9: EOS_PHASE_CHANGE for Liquid Water parameters

MIXTURE	**RLIQ**	**RVAP**	**CLIQ**	**CVAP**	**PSAT**	**V0**
	997.497	0.0205983	1491.03	425	2.81e+3	0.999956

RLIQ: Saturated Liquid's density. *RVAP:* Saturated Vapor's density. *CLIQ:* Speed of Sound for liquid *CVAP:* Speed of Sound for vapor. *PSAT:* Saturated pressure *V0*: Initial relative volume.

Table 10: EOS_PHASE_CHANGE Water Steam parameters

MIXTURE	**RLIQ**	**RVAP**	**CLIQ**	**CVAP**	**PSAT**	**V0**
	997.497	0.0205983	1491.03	425	2.81e+3	48426.18

RLIQ: Saturated Liquid's density. *RVAP:* Saturated Vapor's density. *CLIQ:* Speed of Sound for liquid *CVAP:* Speed of Sound for vapor. *PSAT:* Saturated pressure *V0*: Initial relative volume.

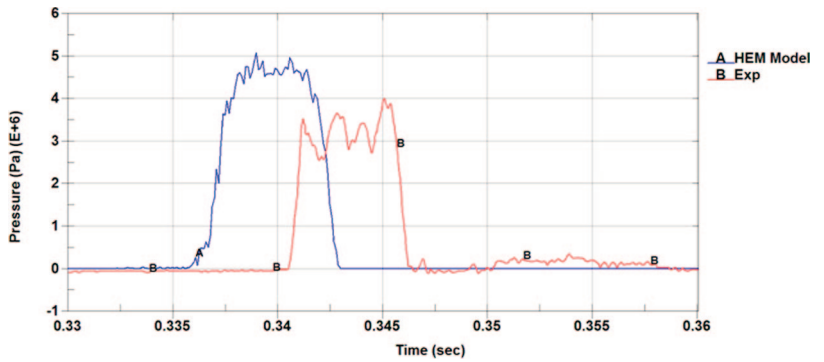

Figure 10: Pressure time history at sensor location (see Figure 9). The blue and red curves represent respectively the LS-DYNA HEM phase-change results and the experimental results

respectively the LS-DYNA HEM phase-change results and the experimental results. The collapse of the vapor pocket occurs at time $t = 0.335$ sec for the numerical simulation and at time $t = 0.343$ sec for the experimental recording, this time difference $\Delta t = 0.005$ sec is very small and can be due to the error in recording during the experience. More importantly one can notice that the implemented phase change model was able to simulate well the phenomenon as the results are well correlated in terms of pressure wave speed propagation (width of the pressure peak) and height.

5. CONCLUSION

In this paper, an equation of state for phase change has been presented in the framework of fluid structure interaction applications. The model has been validated for water hammer problems, where a phase change from liquid to vapor and from vapor to liquid can be generated when the shock pressure reaches the closed valve and being reflected. This problem is very common in nuclear industry, during closing valve for security issues. Nowadays, the coupling with the structure has been solved internally in nuclear industry for one dimensional problem; but has not been published in the literature. In this project, the three dimensional problem has been considered for both fluid and structure, as well as the fluid structure coupling, using contact algorithm at the fluid structure interface. Pressure time history as well as peak pressure are compared to experimental data where good correlation has been observed. Since the HEM one fluid model is a simple model based on density variation, it and can be successfully used for large scale models. For small scale models, a more sophisticated model based on variation of density, pressure and temperature needs to be developed to capture small scale phenomena, mixture and volume fraction of vapor inside an element. Such a model will be developed and used for complex fluid structure interaction problems occurring in nuclear industry.

REFERENCES

[1] Saurel, R., Cocchi, J. P. and Butler, P. B. Numerical Study of Cavitation in the Wake of a Hypervelocity Underwater Projectile, *Journal of Propulsion and Power*, 1999; Vol. 15, No. 4.

[2] Ahuja, V, Hosangadi, A. and Arunajatesan, S. Simulation of cavitation flows using hybrid unstructured meshes, *Journal of Fluids Engineering*, 2001; 123:331–40.

[3] Venkateswaran, S., Lindau, J. W., Kunz, R. F. and Merkle, C. L. Computation of multiphase mixture flows with compressible effects, *Journal of Computational Physics* 2003; 180:54–77.

[4] Senocak, I. and Shyy, W. A pressure-based method for turbulent cavitating flow computations, *Journal of Computational Physics*, 2003; 176:363–83.

[5] Tang, H. S. and Huang, D. A second-order accurate capturing scheme for 1D inviscid flows of gas and water with vacuum zones, *Journal of Computational Physics*, 1996; 128:301–18.

[6] Aanhold, J. E., Meijer, G. J. and Lemmen, P. P. M. Underwater shock response analysis on a floating vessel, *Journal of Shock and Vibration*, 1998; 5:53–9.

[7] Liu, T. G., Khoo, B. C. and Xie, W. F. Isentropic one-fluid modelling of unsteady cavitating flow, *Journal of Computational Physics*, 2004; 201:80–108.

[8] Schmidt, D. P., Rutland, C. J. and Corradini, M. L. A fully compressible, two-dimensional model of small, high speed, cavitating nozzlesn *Journal of Atomization and Sprays*, 1999; 9:255–76.

[9] Barras, G., Souli, M., Aquelet, N. and Couty, N. Numerical simulation of underwater explosions using an ALE method. The pulsating bubble phenomena, *Journal of Ocean Engineering*, 2012; 41:53–66.

[10] Messahel, R., Cohen, B., Souli, M. and Moatammedi, M. Fluid-structure interaction for water hammers effects in petroleum and nuclear plants, *The International Journal of Multiphysics*, 2011; 5:377–4.

[11] Bergerat, L. Développement d'une méthode numérique compressible pour la Simulation de la cavitation en géométrie complexe, *Phd Thesis, ParisTech*, 2012.

[12] Wallis, G. B. One-dimensional two-phase flow, *McGraw-Hill*; 1969.

[13] Simpson, A. R. Large water hammer pressures due to column separation in sloping pipes (transient, cavitation), *PhD Thesis, The University of Michigan*, 1986.

[14] Bergant, A., Simpson, A. R. and Tijsseling, A. S. Water Hammer with column separation: *A review of research in the twentieth century*.

[15] Aquelet, N., Souli, M. and Olovson, L. Euler Lagrange coupling with damping effects: Application to slamming problems, *Computer Methods in Applied Mechanics and Engineering*, 2005, Vol. 195, pp 110–132.

[16] Benson, D. J. Computational methods in Lagrangian and Eulerian hydrocodes, *Computer Methods in Applied Mechanics and Engineering*, 1992; 99:235–394.

[17] Von Neumann, J. and Richtmeyer, R. D. A method for the numerical calculation of hydrodynamical shocks. *Journal of Applied Physics*, 1950; vol. 21, pp. 232.

[18] WAHALoads - Two-phase Flow Water Hammer Transients and Induced Loads on Materials and Structures of Nuclear Power Plants : *WAHA3 Code Manual*.

[19] Hallquist, J.O, LS-DYNA, *Theoretical manual. Livermore Software Technology Corporation, Livermore*, 1998.

[20] Wagner, W. and Pruss, A. The IAPWS Formulation 1995 for the Thermodynamic Properties of Ordinary Water Substance for General and Scientific Use, *J. Phys. Chem. Ref. Data*, 2002, 31; 387–535.

[21] Gale, J. and Tiselj, I. Water Hammer in elastic pipes. *International Conference Nuclear Energy for New Europe*, 2002.

[22] Altstadt, E., Carl, H. and Weiss, R. Fluid-Structure Interaction Investigations for Pipelines. *Technical Report FZR-393, Forschungszentrum Rossendorf,* 2003.

[23] Giot, M., Prasser, H. M., Dudlik, A., Ezsol, G., Habip, M., Lemonnier, H., Tiselj, I., Castrillo, F., Van Hove, W., Perezagua, R. and Potapov, S. Two-Phase Flow Water Hammer Transients and Induced Loads on Materials and Structures of Nuclear Power Plants (WAHALoads). *Technical report, contract FIKS-CT-2000-00106*, 2000.